

Insertion vs. Abstraction in the Reactions of $\text{NH}(\text{a}^1\Delta, v=0, 1)$ with H_2 and D_2

Kumi Yunoki, Atsumu Tezaki,^{*,†} Keiichi Yokoyama,^{††} and Hiroyuki Matsui[†]

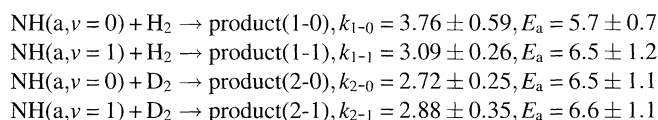
Department of Chemical System Engineering, Faculty of Engineering, The University of Tokyo,
7-3-1, Hongo, Bunkyo-ku, Tokyo 113

[†]Department of Mechanical Engineering, Faculty of Engineering, The University of Tokyo,
7-3-1, Hongo, Bunkyo-ku, Tokyo 113

^{††}Advanced Science Research Center, Japan Atomic Energy Research Institute, Tokai-mura, Naka-gun, Ibaraki 319-11

(Received September 22, 1995)

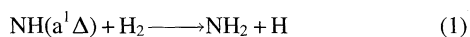
Gas-phase reactions of $\text{NH}(\text{a}^1\Delta, v=0, 1)+\text{H}_2$ (1) and $\text{NH}(\text{a}^1\Delta, v=0, 1)+\text{D}_2$ (2) were studied in the photolysis of HNCO/H_2 (or D_2) mixtures. $\text{NH}(\text{a}^1\Delta)$ and product H (D) atom were detected by UV and vacuum-UV laser-induced fluorescence. The observed rate constants at room temperature (295 ± 2 K) and activation energies in the range of 295—407 K were;



in units of $10^{-12} \text{ cm}^3 \text{ molecule}^{-1} \text{ s}^{-1}$ and kJ mol^{-1} . The product branching ratio in reaction 2 was determined to be $[\text{D}]/[\text{H}] = 3.2 \pm 0.76$, in which no temperature dependence was indicated. These results are consistent with insertion mechanism having a loose entrance transition state structure, which is suggested by ab initio CI calculations. In contrast, the contribution of direct abstraction channel is supposed to be negligibly small.

Chemistry of $\text{NH}(\text{a}^1\Delta)^{1-12)}$ have attracted much interest in comparison with that of the isoelectronic $\text{O}(\text{D})^{13-20)}$ and $\text{CH}_2(\tilde{\text{a}}^1\text{A}_1)^{21-23)}$. Reactions of these singlet biradicals are generally regarded to proceed via insertion into a bond of a counterpart molecule. However, hydrogen abstraction from alkanes by $\text{NH}(\text{a})^{6,7)}$ and $\text{O}(\text{D})^{20)}$ was suggested to compete with the insertion, and physical quenching to ground state triplets can also contribute to the overall decay.^{8,9,23)}

The gas-phase rate constant of



has been well established to be in the range of $2.9\text{--}4.6 \times 10^{-12} \text{ cm}^3 \text{ molecule}^{-1} \text{ s}^{-1}$ at room temperature¹⁻⁴⁾ and the activation energy has been obtained to be $6.4 \pm 0.4 \text{ kJ mol}^{-1}$.¹⁾ In this case, the final products are considered to be the same between insertion and abstraction mechanisms. As well, physical quenching of $\text{NH}(\text{a})$ by H_2 was shown to be far negligible.^{1,4)} In our previous paper,⁴⁾ reaction rate and product branching were analyzed for the reaction



at room temperature. The branching ratio k_{2a}/k_{2b} was de-

termined to be 3.12 ± 0.60 through quantitative analysis of products D and H atoms. The detection of H atom is considered to be a proof of the insertion mechanism since only D atoms can be formed in the abstraction mechanism. Also, as another support for the insertion, vibrational excitation of NH_2 as a product of Eq. 1 was estimated to be close to the statistical distribution.

Theoretical treatments of these reaction paths were conducted by Fueno et al. In their earlier reports using MRD-CI with 4-31G** basis set,^{10,11)} the insertion path was estimated to be barrier-free whereas the abstraction path had a 33 kJ mol^{-1} barrier. However, in Fueno's recent calculation using 6-31G** basis set,¹²⁾ a saddle point of 12 kJ mol^{-1} height was found in the Cs insertion path at 2.0 \AA of N- H_2 distance. On the other hand, the barrier height of the abstraction decreased to 24 kJ mol^{-1} as the level of calculation was raised. Consequently, possibility of the abstraction has not been completely rejected although the dominance of the insertion path seems distinctive.

In this study, we investigate the temperature dependence of the $\text{NH}(\text{a})+\text{H}_2$ (D_2) reactions in order to discuss the possibility of the abstraction further, i.e., product isotopic branching, activation energies of reaction 1 and 2, and the effect of vibrational excitation of $\text{NH}(\text{a})$ on the rate constants are measured.

In addition, ab initio calculations are conducted to characterize the potential energy surface around the transition state (TS) of the possible pathways.

Experimental

All the kinetic information in this experiment was obtained by means of a pump-probe technique in a quasi-static reaction cell. A heating system was additionally equipped to the apparatus that has been previously described.^{4,24} Briefly, a tubular reaction cell (2 cm i.d.) made of Pyrex glass was electrically heated from outside, and the temperature was monitored with a thermocouple that was attached on the cell wall during the kinetic measurements. The gas temperature at the observation point was separately calibrated with another thermocouple inserted in the cell.

$\text{NH}(a, v=0, 1)$ was generated by a pulsed-laser photolysis of HNCN at 193 nm and detected by a laser-induced fluorescence (LIF) technique. The fluence of the photolysis laser was around 10 mJ cm^{-2} at the observation point. $\text{NH}(a, v=0)$ was probed at $\lambda = 325.8 \text{ nm}$ (P_2 line of $c^1\Pi - a^1\Delta$; $0' - 0''$ transition) and $\text{NH}(a, v=1)$ was probed at $\lambda = 363.5 \text{ nm}$ (P_2 line of $c^1\Pi - a^1\Delta$; $0' - 1''$ transition).

H and D atoms were detected by a vacuum-UV (VUV) LIF in the Lyman- α region. The VUV pulse was generated by a frequency tripling, where a dye laser beam at around 364.8 nm was focused with a quartz lens ($f=5 \text{ cm}$) into an adjacent cell filled with Kr at a pressure of 100 Torr. (1 Torr=133.32 Pa) The VUV intensity was calibrated by monitoring ionization current in the downstream section filled with 2% NO diluted in He at 40 Torr.

The fluorescence signals were detected with photomultipliers set perpendicular to the incident laser beams, averaged through a BOXCAR system, and stored in a personal computer. A solar-blind photomultiplier (Hamamatsu R972) was used without optical filters for the detection of VUV fluorescence.

Total pressure in the cell was monitored with a capacitance manometer (MKS Baratron). The partial pressure of HNCN was in the range of 0.4–5 mTorr and the total pressure of the He buffered mixture was maintained at 20 Torr.

HNCN was synthesized and purified as previously.²⁵ Research grade H_2 (99.9999%, Nippon-Sanso) and D_2 (99% isotopic purity, Nippon-Sanso) were used without further purification.

Experimental Results

Rate constants of reactions 1 and 2 as well as product branching ratio of $[\text{D}]/[\text{H}]$ for reaction 2 were measured in the temperature range of 294–407 K.

Overall rate constants were determined from pseudo-first-order analysis of the decay rate of $\text{NH}(a)$. An example of the analysis at room temperature ($295 \pm 2 \text{ K}$) is shown in Fig. 1. Arrhenius descriptions for the temperature dependence of reactions 1 and 2 are shown in Fig. 2. The rate constants at room temperature and the Arrhenius parameters thus obtained are summarized in Table 1. Here, the rate constants of $\text{NH}(a, v=1)$ are nearly equal to those of $\text{NH}(a, v=0)$ for both reactions 1 and 2 and the slight differences between reactions lie within experimental error limits as a whole. Consequently it is reasonable to conclude that there is no remarkable acceleration of the reaction by the vibrational excitation of $\text{NH}(a)$ to $v=1$ although the vibrational energy exceeds the reaction barrier. There seems negligible contribution of vibrational relaxation to the consumption of $\text{NH}(a, v=1)$, because it is unlikely that relaxation rate in H_2 is higher than that in He

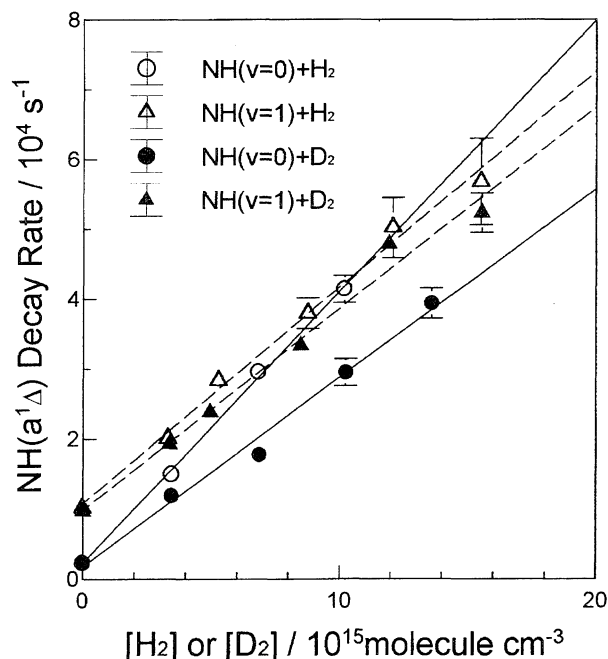


Fig. 1. Pseudo-first-order plots of the decay rate of $\text{NH}(a^1\Delta, v=0, 1)$ in the presence of H_2 or D_2 . $[\text{HNCN}]_0 = 1 \text{ mTorr}$ for the measurements of $\text{NH}(a, v=0)$ and 5 mTorr for $\text{NH}(a, v=1)$.

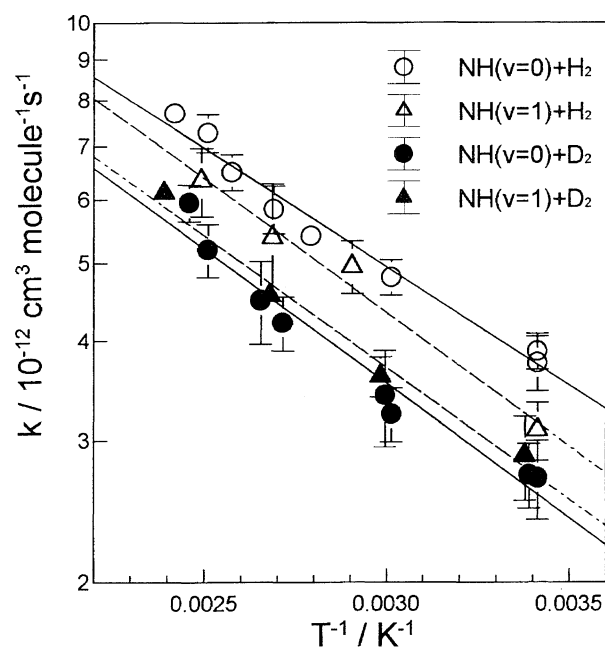


Fig. 2. Arrhenius plots of the reaction rate constants for $\text{NH}(a, v=0, 1) + \text{H}_2$ and $\text{NH}(a, v=0, 1) + \text{D}_2$. $[\text{HNCN}]_0 = 1 \text{ mTorr}$ for the measurements of $\text{NH}(a, v=0)$ and 5 mTorr for $\text{NH}(a, v=1)$.

($< 10^{-14} \text{ cm}^3 \text{ molecule}^{-1} \text{ s}^{-1}$) by more than 2 orders. Reactions 1 and 2 appeared to have almost the same activation energies $E_a \approx 6.3 \text{ kJ mol}^{-1}$, which are also in good agreement with that of the previous study for reaction 1.¹⁾

Figure 3 shows the branching ratio $[\text{D}]/[\text{H}]$ in reaction 2 as a function of temperature. As described in the former paper,⁴⁾ the branching ratio was determined by comparing integrated

Table 1. Summary of the Kinetic Measurements in the reactions (1) $\text{NH(a)}+\text{H}_2$ and (2) $\text{NH(a)}+\text{D}_2$

	$k(295\text{ K})/10^{-12}$ $\text{cm}^3\text{ molecule}^{-1}\text{s}^{-1}$	E_a kJ mol^{-1}	$A/10^{-11}$ $\text{cm}^3\text{ molecule}^{-1}\text{s}^{-1}$	Ref.
$\text{NH(a}, \nu=0)+\text{H}_2$	$3.76 \pm 0.59^{\text{a}}$	5.7 ± 0.7	3.86 ± 0.20	This work
$\text{NH(a}, \nu=1)+\text{H}_2$	3.09 ± 0.26	6.4 ± 0.4	6.8 ± 0.20	1
$\text{NH(a}, \nu=0)+\text{D}_2$	2.72 ± 0.25	6.5 ± 1.2	4.53 ± 0.11	This work
$\text{NH(a}, \nu=1)+\text{D}_2$	2.88 ± 0.35	6.5 ± 1.1	3.62 ± 0.20	This work
		6.6 ± 1.1	4.02 ± 1.05	This work

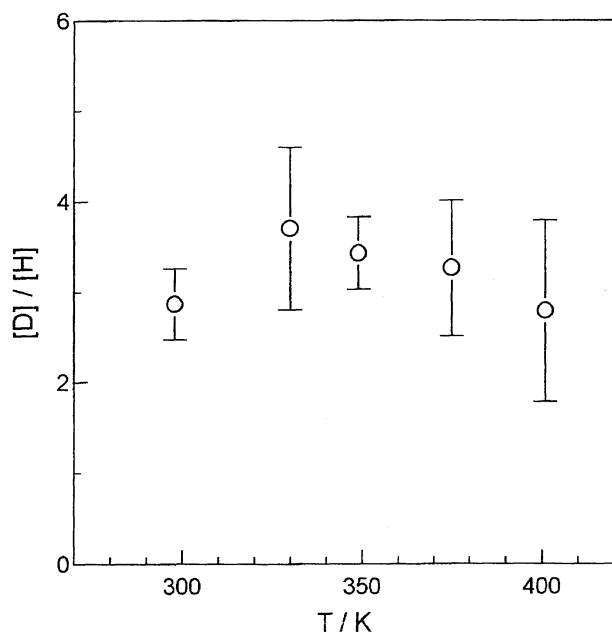
a) Errors indicate 2σ limits.

Fig. 3. Temperature dependence of the product branching ratios of H and D atoms in the reaction $\text{NH(a)}+\text{D}_2$. $[\text{HNCO}]_0=5\text{ mTorr}$ and $[\text{D}_2]_0=0.6\text{ Torr}$ throughout the temperature range. Spectra of H and D were traced at 150 μs after the photolysis and compared with those obtained without D_2 .

line strengths of D and H, which were traced repeatedly at a fixed delay time (at the maximum atomic concentrations) after the photolysis of HNCO/D_2 mixture. Intensity of H atom obtained without D_2 , which consists of initially produced H atom as a branching product of HNCO photolysis, was subtracted from that with D_2 . The average branching ratio was obtained to be;

$$[\text{D}]/[\text{H}] = k_{2a}/k_{2b} = 3.20 \pm 0.76(2\sigma).$$

or,

$$k_{2a}/k_2 = 0.76 \pm 0.05 \text{ and } k_{2b}/k_2 = 0.24 \pm 0.05.$$

Thus, temperature dependence of the branching ratio was not indicated within experimental accuracy. This ratio agrees well with the former result at room temperature of $[\text{D}]/[\text{H}]=3.12 \pm 0.60$.⁴⁾ The populations of the vibrational excited states of NH(a) relative to the ground state in the photolysis of HNCO at 193 nm are reported to be 0.26 ± 0.05 and 0.031 ± 0.010 for $\nu=1$ and $\nu=2$, respectively.²⁶⁾ Since they cannot be discriminated kinetically, the product branch-

ing measured in this study is a combined result from these vibrational states.

Ab initio Calculation

The $^1\Delta$ state of NH has two types of electronic structure of open- and closed-shell characters.¹¹⁾ The open-shell character is that of a biradical in which degenerating π orbitals are singly occupied, i.e., $(\pi)^1(\pi)^1$, and the closed-shell structure is described as a superposition state of two electronic configurations $(\pi)^2(\pi')^0$ and $(\pi)^0(\pi')^2$ combined with a negative sign. In the reaction with H_2 , following overlap relations between the π orbitals and σ or σ^* orbital of the H-H bond are speculated.

(1) Abstractions would take "end-on approach," which means nearly collinear approach from the outside of the bond. The singly occupied π orbital would attack the σ^* orbital at the first stage of the reaction.

(2) Insertions would take "perpendicular approach" to the H-H bond. The doubly occupied π orbital could overlap with the σ^* orbital and the vacant π orbital could overlap with the σ orbital. To confirm these speculations and to determine which approach is favorable in computations, ab initio molecular orbital calculations were performed.

The multi-reference single- and double-excitation configuration interaction (MRCI) method was employed²⁷⁾ to calculate potential energies of the lowest two singlet states in the saddle point region for the abstraction and insertion mechanisms. Higher excitation effect was included by the Davidson correction²⁸⁾ in searching saddle points. Widmark's atomic natural orbital basis sets²⁹⁾ were used with contractions of $[4s3p2d1f]$ for N and $[3s2p1d]$ for H. Reference wave functions were generated from the complete active space self consistent field (CASSCF) procedure with seven active orbitals accommodating eight electrons. Configuration state functions (CSF) with $|c_i| > 0.05$ were selected as reference CSF's, where c_i is the CI coefficient of the i -th CSF. In the present calculation, 11 CSF's were taken as the reference.

We firstly located a saddle point for the abstraction with a restriction of geometry in a plane. A six dimensional parabolic function was fitted to MRCI energies of 246 points to determine the saddle point geometry. The structure of the planar saddle point is depicted in Fig. 4, which agrees well with that calculated by Fueno et al.¹¹⁾ The total energy was calculated to be -56.24559 hartree. Taking the asymptotic energy of -56.25320 hartree into account, the barrier height is determined as 20 kJ mol^{-1} without vibrational zero point

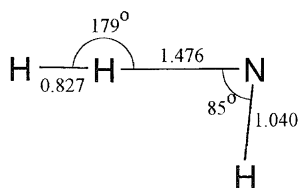


Fig. 4. Saddle point structure on the potential energy surface for planar abstraction obtained in the present MRCI calculation. The nuclear distance is given in Angstrom unit.

energies.

This planar structure, however, is not a true TS. The potential energy was found to decrease when H_2 is rotated around its center, X, in a plane perpendicular to the X-N-H plane. Figure 5 shows the angular dependence of the electronic structures (top) and adiabatic potential energies (bottom) for the lowest two singlet states. Here, we define an index, χ , as a measure of the open-shell character.

$$\chi^2 = c_{11}^2 / (c_{11}^2 + c_{20}^2 + c_{02}^2)$$

where c_{11} , c_{20} , and c_{02} are CI coefficients for electronic configurations $(10a_1)^1(11a_1)^1$, $(10a_1)^2(11a_1)^0$, and $(10a_1)^0(11a_1)^2$, respectively. When χ^2 is, for example, 1.0, the electronic structure has a totally open-shell character.

The curve of χ^2 for the lowest singlet state show that the open-shell character is dominant in the end-on approach and the closed-shell character is dominant in the perpendicular approach. At $\theta=8^\circ$ the electronic character changes. This result is consistent with the intuitive expectation as mentioned above, that is, the abstraction (open shell) mechanism would occur by the end-on approach and the insertion (closed shell) mechanism would occur by the perpendicular approach. The

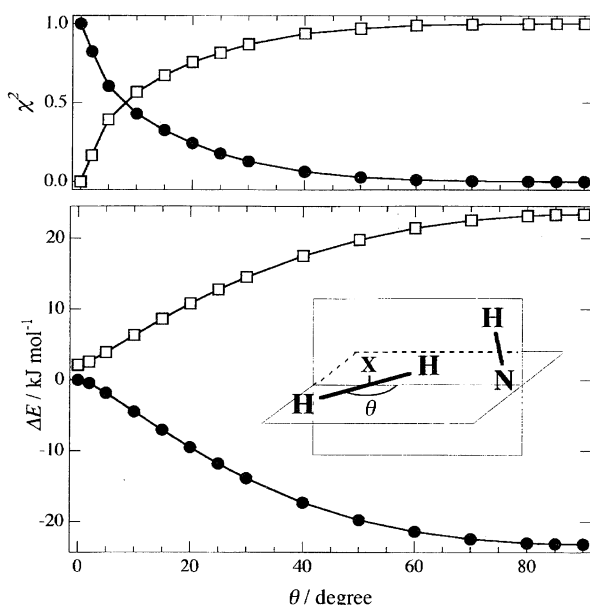


Fig. 5. Angular dependence of the electronic structure and potential energy for the two lowest singlet states. ΔE is measured from the planar saddle point for the abstraction. For the definition of χ , see text. The angle $\theta=0^\circ$ corresponds to the planar saddle point.

second lowest state exhibits complimentary behavior to the lowest state.

The energy minimum shown in Fig. 5 does not mean the correct insertion barrier, since the geometry is not optimized. We attempted to determine the insertion TS with a restriction of the geometry in C_s symmetry, where H_2 molecular axis is normal to the symmetry plane. However, the C_s saddle point was also found to be an energy maximum in a symmetry-breaking mode of vibration and the true TS looks slightly deviated from the correct perpendicular approach. Nevertheless, it is obvious that the nitrogen atom favors to attack H_2 at the side to form a complex than to abstract a hydrogen atom collinearly.

Discussion

The present experimental findings are summarized as follows.

(1) The product branching ratio k_{2a}/k_{2b} showed no temperature dependence in the range 294–407 K. This seems a direct evidence that H (D) is produced mainly by the insertion reaction, except that the activation energy for the abstraction is indistinguishably close to that for insertion.

(2) The activation energies for $\text{NH}(a)+\text{H}_2$ and $\text{NH}(a)+\text{D}_2$ are equal in spite of the lower absolute rates for D_2 than those for H_2 . This seems consistent with the loose TS for insertion, where the distance between N atom and the center of H_2 is rather long (2.0 Å). Frequency shift of H–H vibration is expected to be very small for such a loose structure. The zero-point energies relevant to the H–H (D–D) local vibration, therefore, will not cause an apparent isotope effects on the activation energies. The observed isotopic ratio of the rate constant $k_2/k_1=0.72$ simply reflects the ratio of collision frequencies, which is equivalent to $[\mu(\text{NH}-\text{D}_2)/\mu(\text{NH}-\text{H}_2)]^{-1/2}=0.75$. On the other hand, if the abstraction takes place through the saddle point shown in Fig. 4, the H–H distance at that point is considerably longer than the original distance of 0.75 Å. This implies that the frequency of H–H vibration as well as the zero-point energy should be lowered at the TS. In such a case, the activation energy will increase when H_2 is replaced by D_2 .

(3) The vibrational excitation of $\text{NH}(a)$ into $v=1$ does not accelerate the reaction. This seems consistent with the loose TS for insertion, where incoming translation is the only effective motion to pass the barrier. As shown in Fig. 4, however, present theoretical calculation shows that NH vibrational motion is nearly perpendicular to the reaction path for the abstraction. Thus, effective increase of the reaction rate is not expected by the vibrational excitation of NH for either channel.

There are some cases that vibrational excitation decreases reaction rates such as $\text{CO}(v)+\text{OH}$ and $\text{HCO}(010)+\text{O}_2$.^{30,31)} This negative vibrational effect has been explained with the mechanism that a backward reaction from the intermediate complex is enhanced by the internal energy increase. It is required that the backward potential barrier is higher than the forward one leading to the final products. At the same time, they have to be so close that a considerable amount of

the intermediate can proceed the backward reaction. In the present reaction, however, the exit channel $\text{H}+\text{NH}_2$ is highly exothermic to the initial $\text{NH}(\text{a})+\text{H}_2$ (117 kJ mol^{-1}) so that no backward process from the NH_3 complex is expected. Therefore it should not be the case of the negative vibrational effect although the present experiment showed slight decrease in the rate of $\text{NH}(\text{a},\nu)+\text{H}_2$.

On the well-investigated $\text{O}(^1\text{D})+\text{H}_2$ reaction, the predominance of insertion mechanism seems conclusive after a series of discussion.^{13–19)} That is, reactive cross section, energy partitioning in the products, and their isotope effects have been successfully reproduced by the trajectory calculations conducted on ab initio PES's. In particular, moderately excited, near-statistical vibrational distribution and inverted rotational distribution in the product OH were characteristics of the fast cleavage of the complex formed via insertion. There remain minor discrepancies among the model PES's partly due to the analytical fitting procedure.^{32,33)} Nevertheless, it was shown that abstraction hardly contributes to the overall reaction even on the PES that is most favorable to this channel.^{15,18)} While strictly collinear collision is necessary for the abstraction to occur, most collisions entering inside the threshold impact parameter fall into the deep well of H_2O . Moreover, a barrier of a few kJ mol^{-1} was found in a detailed analysis of the collinear minimum energy path using an ab initio CI calculation.¹⁷⁾

$\text{NH}(\text{a})+\text{H}_2$ reaction has lower rate than $\text{O}(^1\text{D})+\text{H}_2$ owing to the small but non-zero barrier, though, the reaction mechanism appears to be quite similar each other. Also, the vibrational distribution in the product NH_2 was evaluated to be near-statistical in the previous work.⁴⁾ In conclusion, the experimental findings and the theoretical examination of the PES character support that the reaction has a single TS leading to insertion, rather than the competition of the two pathways, at least, over the temperature range of this experiment.

References

- 1) J. W. Cox, H. H. Nelson, and J. R. McDonald, *Chem. Phys.*, **96**, 175 (1985).
- 2) R. D. Bower, M. T. Jacoby, and J. A. Blauer, *J. Chem. Phys.*, **86**, 1954 (1987).
- 3) F. Freitag, F. Rohrer, and F. Stuhl, *J. Phys. Chem.*, **93**, 3170 (1989).
- 4) A. Tezaki, S. Okada, and H. Matsui, *J. Chem. Phys.*, **98**, 3876 (1993).
- 5) H. H. Nelson, J. R. McDonald, and M. H. Alexander, *J. Phys. Chem.*, **94**, 3291 (1990).
- 6) O. Kajimoto and T. Fueno, *Chem. Phys. Lett.*, **80**, 484 (1981).
- 7) O. Kondo, J. Miyata, O. Kajimoto, and T. Fueno, *Chem. Phys. Lett.*, **88**, 424 (1982).
- 8) W. Hack and A. Wilms, *J. Phys. Chem.*, **93**, 3540 (1989).
- 9) W. Hack and K. Rathmann, *J. Phys. Chem.*, **94**, 3636 (1990).
- 10) T. Fueno, V. Bonacic-Koutecky, and J. Koutecky, *J. Am. Chem. Soc.*, **105**, 5547 (1983).
- 11) T. Fueno, O. Kajimoto, and V. Bonacic-Koutecky, *J. Am. Chem. Soc.*, **106**, 4061 (1984).
- 12) T. Fueno, private communication.
- 13) J. A. Davidson, H. I. Schiff, G. E. Streit, J. R. McAfee, A. L. Schmeltekopf, and C. J. Howard, *J. Chem. Phys.*, **67**, 5021 (1977).
- 14) G. K. Smith and J. E. Butler, *J. Chem. Phys.*, **73**, 2243 (1980).
- 15) S. W. Ransome and J. S. Wright, *J. Chem. Phys.*, **77**, 6346 (1982).
- 16) K. Tsukiyama, B. Katz, and R. Bersohn, *J. Chem. Phys.*, **83**, 2889 (1985).
- 17) G. Durand and X. Chapuisat, *Chem. Phys.*, **96**, 381 (1985).
- 18) M. S. Fitzcharles and G. C. Schatz, *J. Phys. Chem.*, **90**, 3634 (1986).
- 19) J. E. Butler, G. M. Jursich, I. A. Watson, and J. R. Wiesenfeld, *J. Chem. Phys.*, **84**, 5365 (1986).
- 20) A. C. Luntz, *J. Chem. Phys.*, **73**, 1143 (1980).
- 21) M. N. R. Ashfold, M. A. Fullstone, G. Hancock, and G. W. Ketley, *Chem. Phys.*, **55**, 245 (1981).
- 22) A. O. Langford, H. P. Petek, and C. B. Moore, *J. Chem. Phys.*, **78**, 6650 (1983).
- 23) U. Bley and F. Temps, *J. Chem. Phys.*, **98**, 1058 (1993).
- 24) M. Koshi, F. Tamura, and H. Matsui, *Chem. Phys. Lett.*, **173**, 235 (1990).
- 25) K. Yamasaki, S. Okada, M. Koshi, and H. Matsui, *J. Chem. Phys.*, **95**, 5087 (1991).
- 26) W. Hack and Th. Mill, *J. Phys. Chem.*, **95**, 4712 (1991).
- 27) B. O. Roos and P. E. M. Siegbahn, "Method of Electronic Structure Theory," ed by H. F. Schaefer, III, Plenum, New York (1977), p. 277.
- 28) S. R. Landghoff and E. R. Davidson, *Int. J. Quantum Chem.*, **8**, 61 (1974).
- 29) P.-O. Widmark, P.-Å. Malmqvist, and B. O. Roos, *Theor. Chim. Acta*, **77**, 291 (1990).
- 30) T. Dreier and J. Wolfrum, "Eighteenth Symposium (International) on Combustion," The Combustion Institute, Pittsburgh, 1981, Abstr., p. 801.
- 31) A. O. Langford and C. B. Moore, *J. Chem. Phys.*, **80**, 4204 (1984).
- 32) R. Schinke and W. A. Lester, Jr., *J. Chem. Phys.*, **72**, 3754 (1980).
- 33) J. N. Murrell and S. Carter, *J. Phys. Chem.*, **88**, 4887 (1984).